

# Behaviour of an annular flow in the convergent section of a Venturi meter

G. Salque<sup>1</sup>, P. Gajan<sup>2</sup>, A. Strzelecki<sup>2</sup> & J. P. Couput<sup>1</sup>

<sup>1</sup>*TOTAL, Allocation and metering group, Pau, France*

<sup>2</sup>*Office National d'Etudes et de Recherches Aéronautiques, Models for Aeronautics and Energetics Department, Toulouse, France*

## Abstract

This paper concerns the flow metering of wet gas by a Venturi meter. In many industrial applications dealing with the gas production, annular/dispersed two phase flows are mainly observed. A theoretical approach based on mass and momentum exchange permits prediction of the pressure, droplet velocity and film thickness distributions between the upstream and the downstream pressure taps. To improve these models, an experimental work dealing with the wall film thickness distribution in the convergent part of the Venturi meter is undertaken from flow visualizations and film thickness measurements. Averaged film thickness and wave characteristics in the convergent section are quantified and compared to theoretical results.

*Keywords: Venturi meter, convergent section, annular flow, liquid film, thickness, interface waves, resistive probes.*

## 1 Introduction

Liquid films flowing on solid surfaces may be observed in different fields (medicine, agriculture, automotive, spatial and aeronautics industry, energy plants, petrol and gas industry etc). Their behaviours were largely studied since few decades. Nevertheless, as far as we know, it seems that no work was published concerning the influence of a longitudinal pressure gradient. This is the case in a Venturi meter used to measure the gas and liquid production of natural reservoirs. When the gas is brought up to surface, condensation



phenomena occur and a liquid phase appears, formed from condensates and water. In many cases the gas volume fraction (GVF) is higher than 95% (wet gas), and the flows encountered are of an annular dispersed type.

Recently, the modelling of the mass and momentum exchanges between the gas and the liquid phases was done in order to calculate the over reading differential pressure induced by the liquid phase (Lupeau et al [1]). The use of this model shows that the liquid film thickness plays an important role on the Venturi meter behaviour. So, it seems important to verify that the liquid film patterns in the meter are accurately taken into account in the calculations.

In this paper, an experimental work developed to analyse the liquid film behaviour in the convergent section of the meter is presented. Two techniques were used; the first based on visualizations gives a qualitative information of the liquid film characteristics, while the second based on resistive measurements permits to quantify the longitudinal distributions.

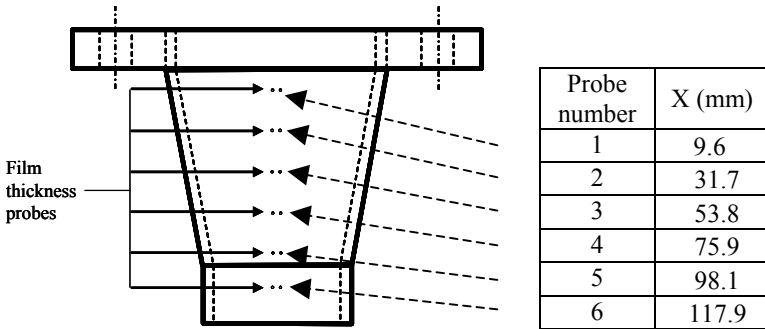


Figure 1: Sketch of the model used to study the liquid film behaviour in the convergent section.

## 2 Experimental set up

### 2.1 Test rig

The tests were carried out at low pressure on the ONERA experimental flow loop. The gas flow (air) is generated by means of high pressure tanks. The gas flow rate is controlled by a sonic nozzle. The mass flow rate of liquid (water) is measured with electromagnetic flow meters. The experiments were performed at atmospheric pressure. The test section is placed in a vertical downwards orientation. It is composed of a flow conditioner, a liquid film injector, and a Venturi meter. The pipe diameter ( $D = 2.R$ ) is 100 mm. For flow visualizations, a Venturi flow meter with a  $\beta$  of 0.6 was machined in Perplex. The half angles of the upstream convergence and the downstream diffuser were respectively  $10.5^\circ$  and  $7.5^\circ$ . The film thickness measurements were performed on a new model including only the convergent section and half of the throat section of the meter. This new device is equipped with six film thickness probes (figure 1).

## 2.2 Experimental techniques used for analysing the film behaviour

Two different techniques are used to analyse the film behaviour. For flow visualizations, an argon laser sheet parallel to the pipe axis is used to illuminate the film and the images are recorded by a CCD camera placed perpendicular to the laser sheet.

The film thickness is determined from a film conductance method described by Hewitt [2]. It consists of measuring the electric impedance between two flush-mounted electrodes. The geometry of the probe (pin diameter  $d$  and pin spacing  $s$ ) depends on the thickness range to be explored (Hewitt et al [3]). Here,  $s/d = 4$  with a pin diameter equal to 1 mm. Each pair of electrodes is connected to an electric circuit to measure the conductance and, after a calibration procedure, the instantaneous thickness. After a signal processing, the average film thickness, the wave amplitude the speed of the superficial waves and their wavelength are deduced.

## 3 Modelling of the gas liquid interaction inside the Venturi meter

To simulate the two phase flow phenomena inside a Venturi meter, it is necessary to take into account the gas/liquid film interaction near the wall, the gas/droplet interaction in the core region and also the mass flux of liquid exchanged between the film and the spray (entrainment and deposition of droplets). Two and three-dimensional calculations of this two phase flow can be considered to take into account the gas liquid interactions of the core region (droplets) [4], but even if recent developments exist to simulate the flow phenomena in the liquid film region (Volume Of Fluid (VOF) [5] or level set techniques [6]), the high grid refinement needed in the three spatial directions does not permit to follow this modelling option. An alternative approach initially developed for a Venturi scrubber has been followed by Azzopardi and co-workers [7]. They use a one-dimensional approach to describe the momentum exchanges between the gas and the liquid phase along the Venturi meter.

The same approach is used by Lupeau et al [1]. The flow is divided into two regions: the convergent section and the throat. In each zone, integrated balance equations (mass and momentum conservation) are applied on the gas flow, the liquid film and the dispersed flow. In each pipe section, each flow is defined by its local velocity  $V$  and its flowing area  $S$ . In these equations, source terms are used to describe the momentum and mass exchanges. This concerns the momentum gas/liquid film interaction at the interface, the momentum exchange between the gas and droplets and the mass exchange between the film and the droplets due to the entrainment. The model supposes that no mass exchange between the liquid and the gas occurs in the meter (evaporation and condensation).

The momentum transfer between the film and the gas is described through the interfacial stress  $\tau_i$  modelled by the Wallis correlation. An atomization of the liquid film is taken into account at the convergent/throat junction. Different



correlations are proposed to estimate the atomised mass flow rate (Fernandez Alonso et al [8]). Lupeau et al [1] used a correlation deduced from a weighting measurement of the liquid film upstream and downstream of the Venturi. The size of the droplet newly atomized at the throat entrance are defined from an empirical correlation (Azzopardi and Govan [9]) and their initial velocity is equal to the average liquid film velocity at the end of the convergent section.

This code permits to calculate the distribution of the pressure, the film thickness and the droplets velocity from the inlet of the meter to its throat section.

## 4 Experimental results

### 4.1 Visualization of the liquid film behaviour through the Venturi meter

Visualizations of the liquid film through the Venturi meter (Lupeau et al [1]) show that the film behaviour mainly depends on the location and on the liquid volume flow rate  $Q_{vl}$ . As a matter of fact, even if an amplification of the disturbance is observed when the gas volume flow rate  $Q_{vg}$  is increased, the influence of the gas velocity does not seem to be the main parameter. On the contrary, the film characteristics change greatly when the liquid flow rate is increased. This can be illustrated by figure 2 which presents different snapshots of the liquid film obtained upstream of the Venturi meter for one gas velocity condition and different liquid flow rates. At low liquid flow rate, the liquid interface is formed of regular small amplitude waves associated with relatively large wavelengths.

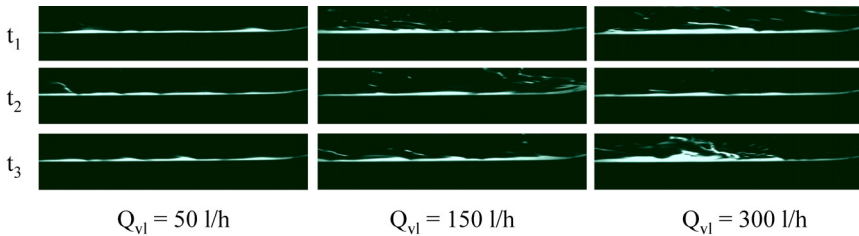


Figure 2: Snapshots of the liquid film upstream of the convergent section ( $Q_{vg} = 630 \text{ m}^3/\text{h}$ ;  $Re_D = 14 \cdot 10^4$ ).

When the liquid flow rate is increased, the amplitude of the waves increases and intermittent large waves, up to 4 times the averaged film thickness, are observed on the movies. On their periphery, liquid ligaments are formed which can induce the entrainment of liquid packets in the gas region and the formation of droplets (Azzopardi et al [10]).

In the convergent part of the meter, the gas acceleration induces a diminution of the wave amplitude and a flattening of the film. Nevertheless, the movies reveal instantaneous breaking of waves linked to entrainment. For the higher liquid flow rates tested, an intermittent appearance of large waves is observed.

At the end of the convergent section, the waves seem to be disorganised. At the throat section, the film becomes thicker and the wavelength greatly diminishes (figure 3). Close to the interface, the number of liquid filaments increases. For the higher liquid flow rates, intermittent large waves are often noticed linked to high entrainment processes. When the film flows through the diffuser, the amplitude of the disturbances decreases and the wavelength increases. The appearance of large waves is still observed at high liquid flow rate.

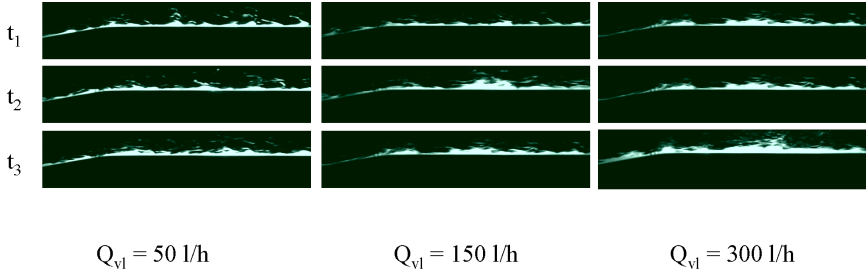


Figure 3: Snapshots of the liquid film at the end of the convergent section ( $Q_{vg} = 440 \text{ m}^3/\text{h}$ ;  $Re_D = 10.7 \cdot 10^4$ ).

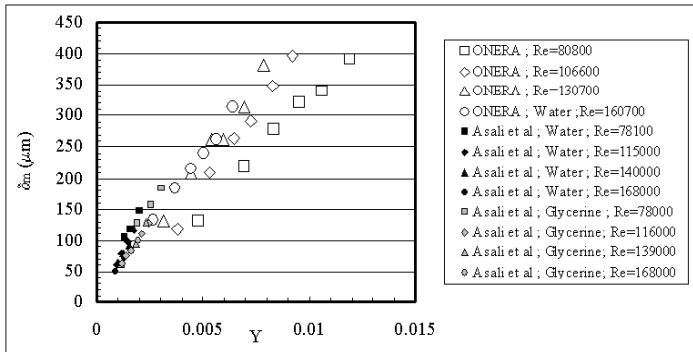


Figure 4: Influence of the flow parameters on the upstream liquid film thickness.

## 4.2 Film thickness measurements

### 4.2.1 Film behaviour upstream of the convergent section

The behaviour of the liquid film upstream from the meter was presented by Lupeau et al [1]. From a simple model, it was shown that the averaged film thickness is proportional to a length scale  $Y$  taking into account the liquid flow rate, the gas velocity, the gas and liquid viscosity, the gas density and the pipe radius.

$$\delta_m = \alpha \cdot \frac{\sqrt{\mu_l Q_{v\_film}}}{(\rho_g R)^{\frac{3}{8}} U_g^{\frac{7}{8}} \mu_g^{\frac{1}{8}}} = \alpha Y \tag{1}$$

In Figure 4,  $\delta_m$  variation with respect to  $Y$  is plotted and compared to the data given by Asali and Hanratty [11]. This graph shows that the  $Y$  parameter correlates the results of Asali and Hanratty [11] obtained for different flow conditions and different liquids. In the ONERA case, a scatter of the results is obtained when the air velocity changes. Nevertheless, these results indicate that the film thickness is linearly dependent on the square root of the liquid film flow rate.

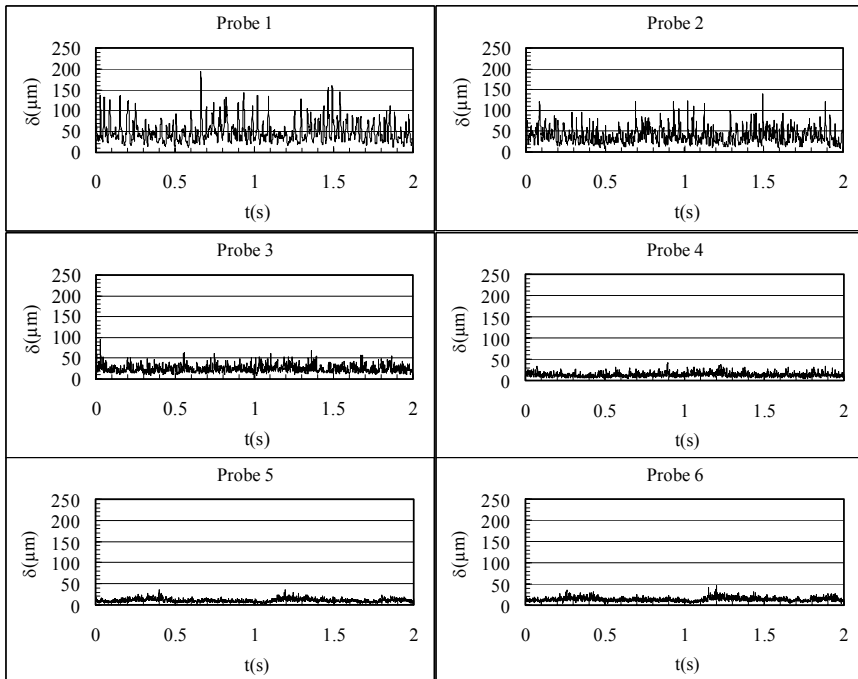


Figure 5: Signals of liquid film thickness inside of the convergent section ( $Q_{vg} = 650 \text{ m}^3/\text{h}$ ;  $Q_{vl} = 50 \text{ l/h}$ ).

#### 4.2.2 Modification of the film characteristics in the convergent section

Typical film thickness signals are presented in figure 5. Close to the convergent section inlet (probe 1), large peaks are observed. As before, their amplitude augments with the liquid flow rate and the signal becomes noisy. As the film flows into the convergent section, these peaks decrease and fluctuations with low amplitude and high frequencies appear.

The average thicknesses computed from these signals are plotted in figure 6. They are compared to distributions predicted by the code. Bold symbols correspond to film thickness measurements performed 1D upstream of the meter. First of all, experimental results indicate that the liquid film thickness increases slightly between the two first probes then decreases inside the convergent section. Comparisons between the upstream location (bold symbol) and the first

probe position indicate that the liquid film flattens at the inlet of the convergent section. This phenomenon can be induced by the transverse pressure gradient linked to the streamline curvature in this region. New experiments are planned to verify this hypothesis. The numerical results only predict a monotone thickness diminution. A great discrepancy appears on the absolute value.

Further treatments are done on the signals in order to determine the amplitude, the convection velocity and the corresponding wavelengths of the longitudinal interfacial waves. In a first step, the wave amplitude evolution is analysed. Such information is used to calculate the interfacial stresses (Giroud-Garapon [13]). In a previous experimental work on liquid film behaviour on a hot inclined plate, Giroud-Garapon [13] obtained the following correlation:

$$\frac{A}{\delta} = 1.136 \cdot \text{Re}_l^{0.111} \left[ 1 - 20.456 * \left( \frac{\tau_g \cdot \delta}{\sigma} \right)^{1.048} \right] \quad (2)$$

In this expression,  $A$  is the amplitude of the wave,  $\text{Re}_l$  is the Reynolds number of the liquid film,  $\tau_g$  is the wall stress in dry gas and  $\sigma$  is the surface tension coefficient. The amplitude of the wave is deduced from the film thickness distribution  $\mathcal{D}(\delta)$  calculated from the thickness probability function  $P(\delta)$ .

$$\mathcal{D}(\delta) = \int_0^{\delta} P(\delta) d\delta \quad (3)$$

$$A = \delta(\mathcal{D} = 99\%) - \delta(\mathcal{D} = 1\%) \quad (4)$$

Comparisons between correlation and measurement results are presented in figure 7. If this correlation gives good results upstream of the plate, it seems that additional phenomena appear in the convergent which amplify the wave oscillations especially at high liquid flow rate.

In a second step, the convection velocity  $U_c$  of the waves is determined from intercorrelations. In upper graph of the figure 8, the acceleration of the waves is observed. It depends on the liquid and gas flow rates.

Figure 5 shows that the waves are divided into two classes, long waves with high amplitude and short waves or ripples with small amplitude. Signal processing was developed to quantify these two wave configurations. The long waves  $\Lambda$  which correspond to high thickness variations are measured from FFT. The small wavelengths  $\lambda$  are deduced from time period histogram. The evolution of these wavelengths in the convergent section is plotted on the lower graphs of the figure 8. It is obvious that the long waves scale  $\Lambda$  is equivalent or larger than the convergent length. So it is expected that these waves cannot be seen as a roughness. A stretching effect is clearly observed. The influence of the gas and liquid flow rates is not obvious. For the higher gas flow rate, the wavelength augments with the liquid flow rate while a non-monotone evolution is obtained for the lower gas flow rate. Further analyses are needed to explain this phenomenon. On the opposite, the size of the ripple waves  $\lambda$  is always inferior to the length of the convergent section. For the higher gas flow rate, this scale diminishes continuously as the film flows into the convergent section. For the lower flow rate, it increases first then decreases quickly. As before, this behaviour has to be analysed in more detail in the future.



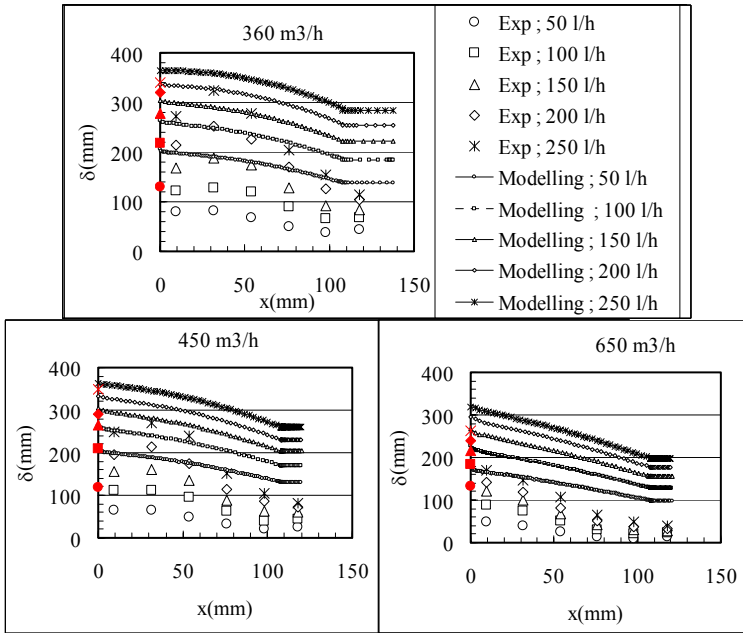


Figure 6: Evolution of the mean film thickness inside of the Venturi meter (bold symbols corresponds to measurements obtained 1D upstream of the convergent section).

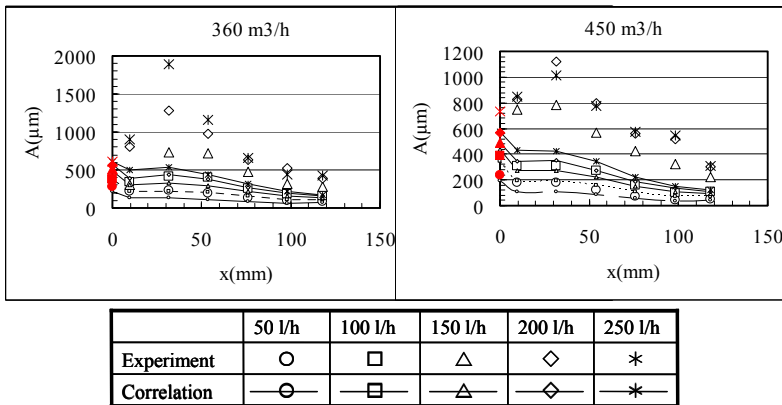


Figure 7: Wave amplitude distribution in the convergent section (bold symbols corresponds to measurements obtained 1D upstream of the convergent section).



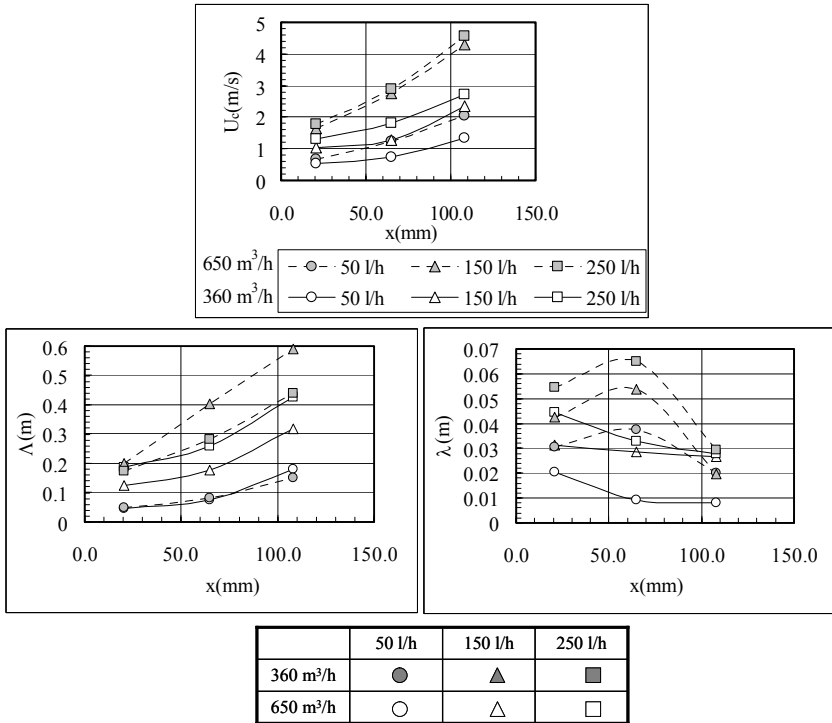


Figure 8: Convection velocity and wavelengths measured at the interface (left: long waves; right: ripples).

## 5 Conclusion

The mass and momentum interactions between the liquid phase and the gas phase have to be accurately modelled in order to calculate the impact of the liquid phase on the differential pressure measured on a Venturi meter used in wet gas condition. Among these different interactions, the behaviour of the liquid film on the pipe wall during its flow in the convergent section has to be studied in detail. For this purpose, a dedicated experiment was performed with air and water at atmospheric pressure. The results are compared with 1D flow modelling. The flattening of the film in the convergent section is shown. Nevertheless a great difference appears with the modelling results which indicates that further phenomena not taken into account in the 1D model, appear. From signal analysis, two types of wave are distinguished (high amplitude waves and ripples). The long waves are stretched in the Venturi and their amplitude diminishes. On the contrary, the ripple wavelengths seem to diminish. Further experiments and data analyses are underway to complete these first observations.

## References

- [1] Lupeau A, Platet B., Gajan P., Strzelecki A., Escande J., Couput J.P. Influence of the presence of an upstream annular liquid film on the wet gas flow measured by a Venturi in a downward vertical configuration. *Flow Meas. and Inst.* 18(1), (2007), 1–11.
- [2] Hewitt G.F., *Measurement of two phase flow parameters*, Academic Press, (1978)
- [3] Hewitt G.F., King R.D., Lovegrove P.C., *Techniques for liquid film pressure drop studies in annular two phase flow*, Rept. AERE-R3921, UKAEA, Harwell, (1962)
- [4] Bissières D, Couput J.P, Estivalezes J.L., Gajan P., Lavergne G., Strzelecki A., *Wet gas flow simulation for venturi meters*, 1<sup>st</sup> North America Conference on Multiphase Technology, Banff, (1998)
- [5] Hirt C. and Nichols B., *Volume of fluid method for the dynamics of free boundaries*, *Journal of Computational Physics*, 39(1), (1981), 201-225
- [6] Osher S., Fedkiw R., *Level Set Methods: An Overview and Some Recent Results*, *Journal of Computational Physics*, 169(2), (2001), 463-502
- [7] van Werven M., van Maanen H. R. E., Ooms G. and Azzopardi B. J., *Modeling wet-gas annular/dispersed flow through a Venturi*, *AIChE Journal*, 49(6), (2003), 1383-1391
- [8] Fernandez Alonso D., Azzopardi B.J., Hills J.H., *Gas/liquid flow in laboratory-scale venturis*, *ICChem*, 77, (1999), 205-211
- [9] Azzopardi B.J., Govan, A.H., *The modeling of Venturi scrubbers*, *Filtration and Separation*, 21, (1984), 196-200
- [10] Azzopardi, B. J., Taylor, S. and Gibbons, D. B. *Annular two-phase flow in large diameter pipes*. *Int. Conf. on Physical Modelling of Multi-Phase Flow*, April 19-21, Coventry, (1983), 267-282.
- [11] Asali J.C., Hanratty T.J., *Ripples generated on a liquid film at high gas velocities*, *Int. J. of Multiphase flows*, 19(2), (1993) 229-243
- [12] Webb D.R., Hewitt G.F., *Downwards co-current annular flow*, *Int. J. of Multiphase flows*, 2, (1975) 35-49.
- [13] Giroud-Garapon S., *Etude du comportement d'un film liquide dans les chambres de combustion de statoréacteurs et/ou turboréacteurs*, PhD Thesis, Ecole Nationale Supérieure de l'Aéronautique et de l'Espace, 2003

